*Liquid Crystals,*
Vol. 37, No. 12, December 2010, 1559–1568

Taylor & Francis
Taylor & Francis Group

# Surface viscosity and reorientation process in an asymmetric nematic cell

Rodolfo Teixeira de Souza*, Ervin Kaminski Lenzi and Luiz Roberto Evangelista

*Departamento de Fisica, Universidade Estadual de Maringá, Avenida Colombo, 5790 87020-900 Maringá - PR, Brazil*

(*Received 24 June 2010; final version received 9 August 2010*)

The influence of surface viscosity and anchoring energy on the reorientation process of a nematic liquid crystal cell is theoretically investigated. The cell is a slab of thickness, $d$, whose limiting surfaces are characterised by different anchoring strengths and present easy directions parallel to the bounding surfaces, changing with time due to some external action. The exact space-time profile of the director angle is obtained by means of integral transform techniques and a Green function approach. From this formalism, the time dependence of the optical path difference is exactly determined and its behaviour is analysed in connection with the presence of surface viscosity and different anchoring energies. The problem is also exactly solved in the presence of a constant electric field. It is shown that the compatibility problem between the time derivative of the director field on the surface and in the bulk can be avoided.

**Keywords:** nematic liquid crystals; reorientation process; surface viscosity; Green function approach



## 1. Introduction

In recent years, several analyses have focused on the role played by the surface viscosity in the dynamical behaviour of nematic liquid crystal (NLC) cells [1–6]. This significant attention of the scientific community is due in part to the importance of the problem in display technology and, to a considerable extent, in view of the important mathematical issues it raises [7–12]. The concept of surface viscosity, introduced by Derzhanskii and Petrov [13] to account for the surface changes of the director with time, together with the concept of anchoring energy, in the Rapini–Papoular sense [14], form the usual framework to understand surface properties connected with relaxation processes of liquid-crystalline samples. In this scenario, the total energy of the sample is composed of the elastic energy corresponding to the deformation and the surface contributions. The surplus of energy due to the presence of the limiting surfaces, known as surface energy, has two contributions. One contribution is related to the broken symmetry of the nematic phase due to the presence of the surface, and is responsible for a reduced interaction of the nematic molecules located in the surface layer whose thickness is smaller than the range of the molecular interactions responsible for the nematic phase (the intrinsic contribution). The other contributions (the extrinsic contribution) is due to the direct interaction between the nematic molecules and the molecules of the substrate [15]. The equilibrium configuration is found by minimising this total energy. From the mathematical point of view, this implies the need to search for solutions of a torque balance equation (bulk) subject to appropriate boundary conditions, if the complete dynamical behaviour is the scope of the analysis. In this regard, the influence of the anchoring energy as well as the surface viscosity on the relaxation process of a nematic cell have been analysed by considering an imposed deformation on the sample [12, 16]. In these works, the molecular orientation–reorientation process in a cell in the shape of a slab of thickness, $d$, composed of two identical surfaces has been analysed. The space-time profile of the director angle has been exactly determined by means of a Green function method [16]. This kind of analysis has lead to the conclusion that in the limit of strong anchoring the influence of the surface viscosity can be considered negligible.

In this paper, we re-examine the mathematical problem discussed in [16] by considering a more general situation in which the surfaces forming the slab are not identical, i.e. by considering the problem of a asymmetric cell having two different anchoring strengths and different time-dependent easy axis distributions, which can be relevant to the phenomenological discussion of light-induced easy directions in doped cells [17, 18]. Our twofold purpose is to analyse the role of the asymmetric distribution of easy axes, with boundary conditions involving the surface viscosity, on the profile of the director angle, and also to formulate the problem in a way that can, more generally than the preceding problems, still be tackled by means of analytical methods even in the presence of

*Corresponding author. Email: rodolfo@dfi.uem.br

ISSN 0267-8292 print/ISSN 1366-5855 online

DOI: 10.1080/02678292.2010.515041
http://www.informaworld.com

a constant electric field applied to the sample. As a result, we offer a complete conceptual tool to obtain the exact results for the profile of the director angle and other experimentally measurable quantities such as the optical path difference, whose exact temporal behaviour can be determined. In our analysis we assume, as has been stated above, that the surface easy axes are changing with time, whereas the anchoring energy strengths related to these easy directions are assumed to be time independent. In this framework, the easy axis is defined as the nematic surface orientation for which the surplus of energy due to the limiting surface reaches its minimum value, for a uniform orientation of the nematic in the bulk. Since we are assuming that the anchoring energy strength is time independent, the orientation of the nematic molecules in the surface layers does not change during the modification of the easy axis. This implies that the easy axes have to be varied mechanically, turning the limiting surfaces with respect to the initial position. To the best of our knowledge, experiments of this type have not been performed until now. We hope that our paper will stimulate research in this direction, thus permitting us to compare our theoretical prediction with the experimental results. Recently, the modification of the easy axes induced by the interaction of the light with nematic liquid crystals doped with dyes has been discussed [17–24]. In these types of experiment, the easy axis is changed by inducing an adsorption and a structural transformation of the dye dissolved in the liquid crystal. The adsorption and the structural transformations of the molecules of dye are related to two different characteristic times. This means that the density of the molecules of the dyes responsible for the anchoring energy, and their orientation that is responsible for the easy axis, change with irradiation time. Consequently, the easy axis *and* the anchoring energy strength change with time [20]. This case cannot be described by means of our theoretical model. An extension of the model to describe the experiment reported in [18] is under way, and will be published elsewhere.

The paper is organised as follows. In Section 2, the statement of the problem is presented, introducing the temporally dependent asymmetric easy axis distributions in such a manner as to mathematically formulate the problem in general terms. In Section 3, the Green function approach is developed to obtain the exact solution for the space-time profile of the director angle. In Section 4, some theoretical results for the time derivative of the director angle and for the optical path difference are presented for a relevant set of parameters characterising a typical NLC sample. In Section 5, the effect of an external, constant, electric field on the relaxation behaviour of the system is considered. Finally, in Section 6, some concluding remarks are presented.

## 2. Statement of the problem

The sample is an NLC cell in the shape of a slab of thickness $d$ in such a manner that the $z$-axis of a Cartesian reference frame is normal to the bounding walls placed at $z = \pm d/2$. The twist angle formed by the nematic director, **n**, with the $x$-axis, characterising the nematic deformation, is indicated by $\phi$, and the one-elastic constant approximation is assumed. The dynamics of the director angle in the cell is governed by the equation arising from the balance condition between the elastic and viscous torque [25]:

$$\eta_{\mathrm{b}} \frac{\partial}{\partial t}\phi(z,t) = K \frac{\partial^2}{\partial z^2}\phi(z,t), \tag{1}$$

where $K$ is the elastic constant and $\eta_{\mathrm{b}}$ is the (effective) bulk viscosity. The equilibrium profile of the director angle has to be found satisfying the boundary conditions stating the elastic torque transmitted by the liquid crystal to the limiting surface is balanced by the restoring torque due to the anisotropic interaction of the nematic molecules with the surface and by the viscous torque, due to the surface dissipation, namely

$$\pm K \frac{\partial}{\partial z}\phi(z,t) + W_{\pm}\left[\phi(z,t) - \phi_{\mathrm{s},\pm}(t)\right] + \eta_{\mathrm{s}} \frac{\partial}{\partial t}\phi(z,t)\bigg|_{z=\pm d/2} = 0, \tag{2}$$

where $\eta_{\mathrm{s}}$ is the surface viscosity [13]. In Equation (2), the parabolic approximation for the Rapini–Papoular surface anchoring energy is assumed, i.e. $f_{\mathrm{s},\pm} = (1/2)W_{\pm}[\phi(t) - \phi_{\mathrm{s},\pm}(t)]^2$, where $W_{\pm}$ (signs + and – refer to the surfaces located at $d/2$ and $-d/2$, respectively) are the anchoring energy strengths [15] and $\phi_{\mathrm{s},\pm}(t)$ are the surface easy axes characterising the two surfaces of the sample. In addition, we assume that the easy axes change with time, due to the presence of an external action [19–24], according to the laws

$$\phi_{\mathrm{s},\pm}(t \le 0) = \phi_{\mathrm{i},\pm}, \quad \text{and}$$
$$\phi_{\mathrm{s},\pm}(t) = \phi_{\mathrm{f},\pm} + (\phi_{\mathrm{i},\pm} - \phi_{\mathrm{f},\pm})e^{-t/\tau_{\pm}}, \tag{3}$$

where i (f) stands for initial (final) and $\tau_{\pm}$ are the typical characteristic times related to the external action on the aligning surfaces. The easy directions of the kind represented by Equation (3) can by mechanically or optically induced in the system. In the case of photo-induced alignment, azo-dye dopants can also come into play and time-dependent variations in the easy directions result from the illumination process

[17, 18]. From Equation (3), it follows that the initial director profile is

$$\phi(z,0) = \mathcal{A}_{\rm i} + \mathcal{B}_{\rm i}\, z. \tag{4}$$

The final form of the director profile may be obtained by considering that $\lim_{t\to\infty}\ \phi_{\rm s,\pm}(t) = \phi_{\rm f,\pm}$ for the boundary conditions, which leads us to the stationary solution, i.e. $\lim_{t\to\infty}\phi(z,\,t) = \phi_{\rm est}(z)$:

$$\phi_{\rm est}(z) = \mathcal{A}_{\rm f} + \mathcal{B}_{\rm f}\, z, \tag{5}$$

with

$$\begin{aligned}\mathcal{A}_{\rm i(f)} &= \frac{u_+\,(1+u_-/2)\,\phi_{\rm i(f),+} + u_-\,(1+u_+/2)\,\phi_{\rm i(f),-}}{u_+\,(1+u_-/2) + u_-\,(1+u_+/2)},\\ \mathcal{B}_{\rm i(f)} &= \frac{2}{d}\,\frac{u_+u_-\left(\phi_{\rm i(f),+} + \phi_{\rm i(f),-}\right)}{u_+\,(1+u_-/2) + u_-\,(1+u_+/2)}\end{aligned} \tag{6}$$

where $u_\pm = W_\pm\, d/K$ are the reduced anchoring energies and $\phi_{\rm i,\pm} = (\phi_{\rm i,+},\, \phi_{\rm i,-})$.

For $t \le 0$, the profile of the director angle is given by Equation (4). Therefore, from Equations (1) and (2), it follows that

$$\left(\frac{\partial\phi}{\partial t}\right)_{\rm surface,t=0} = \left(\frac{\partial\phi}{\partial t}\right)_{\rm bulk,t=0} = 0, \tag{7}$$

i.e. there is no incompatibility between the time derivative of the director angle on the surface evaluated by means of the bulk equation, Equation (1), and by means of the boundary conditions, Equations (2), at $t = 0$, as discussed in [16].

## 3. The Green function approach

To proceed, we write Equations (1) and (2) in the dimensionless form, as usual, to obtain

$$\frac{\partial}{\partial t_{\rm r}}\phi(z_{\rm r},t_{\rm r}) = \frac{\partial^2}{\partial z_{\rm r}^2}\phi(z_{\rm r},t_{\rm r}), \tag{8}$$

and

$$\begin{aligned}\pm\frac{\partial}{\partial z_{\rm r}}\phi(z_{\rm r},t_{\rm r}) + u_\pm[\phi(z_{\rm r},t_{\rm r}) - \phi_{\rm s,\pm}(t_{\rm r})]\\ +\upsilon\frac{\partial}{\partial t_{\rm r}}\phi(z_{\rm r},t_{\rm r})\,\big|_{z_{\rm r}=\pm1/2} = 0,\end{aligned} \tag{9}$$

respectively, with $z_{\rm r} = z/d$, $t_{\rm r} = t/\tau_D, \tau_{\rm r,\pm} = \tau_\pm/\tau_D$ and $\upsilon = \eta_{\rm s}/(\eta_{\rm b}d)$, where $\tau_D = \eta_{\rm b}\ d^2/K$ is the diffusion time. The next step is to use the Laplace transform $\mathcal{L}\{\cdots\} = \int_0^\infty dt_{\rm r}e^{-st_{\rm r}}\cdots$ and $\mathcal{L}^{-1}\{\cdots\} = \frac{1}{2\pi i}\int_{\gamma-i\infty}^{\gamma+i\infty} ds\, e^{st_{\rm r}}\cdots$, and the Green function approach to obtain a solution of Equation (8). This task can be easily accomplished if we consider first an initial condition for Equation (8), $\Phi_0(z) = \phi(z,0)$, given by Equation (4). Laplace transforms of Equations (8) and (9) yield, respectively,

$$\frac{d^2}{dz_{\rm r}^2}\phi(z_{\rm r},s) - s\phi(z_{\rm r},s) = -\Phi_0(z_{\rm r}) \tag{10}$$

and

$$\begin{aligned}\pm\frac{d}{dz_{\rm r}}\phi(z_{\rm r},s) + (u_\pm\ +\ \upsilon s)\phi(z_{\rm r},s)\,\big|_{z_{\rm r}=\pm1/2}\\ = \upsilon\Phi_0(z_{\rm r})\,\big|_{z_{\rm r}=\pm1/2} + u\phi_{\rm s,\pm}(s).\end{aligned} \tag{11}$$

The Green function of the problem related to Equations (10) and (11) is a solution of the differential equation

$$\frac{d^2}{dz_{\rm r}^2}\mathcal{G}(z_{\rm r},z_{\rm r},';s) - s\mathcal{G}(z_{\rm r},z'_{\rm r};s) = \delta(z_{\rm r}-z'_{\rm r}) \tag{12}$$

with boundary conditions

$$\pm\frac{d}{dz_{\rm r}}\mathcal{G}(z_{\rm r},z'_{\rm r};s) + (u_\pm + \upsilon s)\mathcal{G}(z_{\rm r},z'_{\rm r};s)\,\big|_{z_{\rm r}=\pm1/2} = 0. \tag{13}$$

Now, by using the Green function approach the solution of Equation (10) may be written as

$$\begin{aligned}\phi(z'_{\rm r},s) = -\int_{-1/2}^{1/2} dz_{\rm r}\Phi_0(z_{\rm r})\mathcal{G}(z_{\rm r},z'_{\rm r},s)\\ -[\upsilon\Phi_0(z_{\rm r}) + u_+\phi_{\rm s,+}(s)]\mathcal{G}(z_{\rm r},z'_{\rm r},s)\,\big|_{z_{\rm r}=1/2}\\ -[\upsilon\Phi_0(z_{\rm r}) + u_-\phi_{s,-}(s)]\mathcal{G}(z_{\rm r},z'_{\rm r},s)\,\big|_{z_{\rm r}=-1/2}.\end{aligned} \tag{14}$$

After performing integration of the initial condition and the substitution of $z_{\rm r} = -1/2$ in the second term, one has to replace $z'_{\rm r}$ by $z_{\rm r}$, to obtain $\phi(z_{\rm r},s)$, i.e. the director profile in the Laplace space.

The first term present in Equation (14) gives the time evolution of the initial condition, $\Phi_0(z_{\rm r})$, introduced in Equation (10), and the remaining terms are surface terms. To write the solution in this general form is a convenient way to understand how the surface conditions influence the time evolution of the initial condition. After some calculations, it is possible to show that

$$\mathcal{G}(z_{\rm r}, z'_{\rm r}, s) = -\frac{1}{\sqrt{s}\mathcal{F}(s)}\left\{\sqrt{s}\cosh\left[\sqrt{s}\left(\frac{1}{2}+z_{\rm r}\right)\right] + (u_- + \upsilon s)\sinh\left[\sqrt{s}\left(\frac{1}{2}+z_{\rm r}\right)\right]\right\} \times \left\{\sqrt{s}\cosh\left[\sqrt{s}\left(\frac{1}{2}-z'_{\rm r}\right)\right] + (u_+ + \upsilon s)\sinh\left[\sqrt{s}\left(\frac{1}{2}-z'_{\rm r}\right)\right]\right\}, \tag{15}$$

for $-1/2 \leq z_{\rm r} < z'_{\rm r}$, and

$$\mathcal{G}(z_{\rm r}, z'_{\rm r}, s) = -\frac{1}{\sqrt{s}\mathcal{F}(s)}\left\{\sqrt{s}\cosh\left[\sqrt{s}\left(\frac{1}{2}+z'_{\rm r}\right)\right] + (u_- + \upsilon s)\sinh\left[\sqrt{s}\left(\frac{1}{2}+z'\right)\right]\right\} \times \left\{\sqrt{s}\cosh\left[\sqrt{s}\left(\frac{1}{2}-z_{\rm r}\right)\right] + (u_+ + \upsilon s)\sinh\left[\sqrt{s}\left(\frac{1}{2}-z_{\rm r}\right)\right]\right\}, \tag{16}$$

for $z'_{\rm r} < z_{\rm r} \leq 1/2$, where

$$\mathcal{F}(s) = [s + (u_+ + \upsilon s)(u_- + \upsilon s)]\sinh(\sqrt{s}) + \sqrt{s}(u_+ + u_- + 2\upsilon s)\cosh(\sqrt{s}). \tag{17}$$

Equations (14), (15) and (16) represent the solution of Equation (8) in the Laplace space. In order to get the inverse Laplace transform, we need to close a contour of the integral in the complex space on the poles of $\mathcal{F}(s)$ which appear after taking $s = -k_n^2$, leading us to the eigenvalue equation

$$[(u_+ - \upsilon k_n^2)(u_- - \upsilon k_n^2) - k_n^2]\sin(k_n) + k_n(u_+ + u_- - 2\upsilon k_n^2)\cos(k_n) = 0. \tag{18}$$

By performing the inverse Laplace transform of Equations (15) and (16), we obtain

$$\mathcal{G}(z_{\rm r}, z'_{\rm r}; t_{\rm r}) = -\sum_{n=1}^{\infty}\frac{e^{-k_n^2 t_{\rm r}}}{k_n\tilde{\mathcal{F}}(k_n)}\left\{k_n\cos\left[k_n\left(\frac{1}{2}+z_{\rm r}\right)\right] + (u_- - \upsilon k_n^2)\sin\left[k_n\left(\frac{1}{2}+z_{\rm r}\right)\right]\right\} \times \left\{k_n\cos\left[k_n\left(\frac{1}{2}-z'_{\rm r}\right)\right] + (u_+ - \upsilon k_n^2)\sin\left[k_n\left(\frac{1}{2}-z'_{\rm r}\right)\right]\right\}, \tag{19}$$

for $-1/2 \leq z_{\rm r} < z'_{\rm r}$, and

$$\mathcal{G}(z_{\rm r}, z'_{\rm r}; t_{\rm r}) = -\sum_{n=1}^{\infty}\frac{e^{-k_n^2 t_{\rm r}}}{k_n\tilde{\mathcal{F}}(k_n)}\left\{k_n\cos\left[k_n\left(\frac{1}{2}+z'_{\rm r}\right)\right] + (u_- - \upsilon k_n^2)\sin\left[k_n\left(\frac{1}{2}+z'_{\rm r}\right)\right]\right\} \times \left\{k_n\cos\left[k_n\left(\frac{1}{2}-z'_{\rm r}\right)\right] + (u_+ - \upsilon k_n^2)\sin\left[k_n\left(\frac{1}{2}-z'_{\rm r}\right)\right]\right\}, \tag{20}$$

for $z'_{\rm r} < z_{\rm r} \leq 0$, where

$$\tilde{\mathcal{F}}(k_n) = \frac{1}{2k_n}[k_n^2(1 + \upsilon(6 + u_+ + u_- - uk_n^2)) - u_+(1 + u_-) - u_-]\cos(k_n) + \frac{1}{2}[2 + u_+ + u_- + 2(u_+ + u_- - k_n^2) - 4k_n^2\upsilon^2]\sin(k_n). \tag{21}$$

The inverse Laplace transform of Equation (14) is

$$\phi(z'_{\rm r}, t) = -\int_{-1/2}^{1/2} dz_{\rm r}\Phi_0(z_{\rm r})\mathcal{G}(z_{\rm r}, z'_{\rm r}, t) - \upsilon[\Phi_0(z_{\rm r})|_{z_{\rm r}=1/2}\tilde{\mathcal{G}}_+(z'_{\rm r}, t) + \Phi_0(z_{\rm r})|_{z_{\rm r}=-1/2}\tilde{\mathcal{G}}_-(z'_{\rm r}, t)] - \int_0^t dt'[u_+\phi_{{\rm s},+}(t')\tilde{\mathcal{G}}_+(z'_{\rm r}, t-t') + u_-\phi_{{\rm s},-}(t')\tilde{\mathcal{G}}_-(z'_{\rm r}, t-t')], \tag{22}$$

with $\tilde{\mathcal{G}}_\pm(z'_{\rm r}, t_{\rm r}) = \mathcal{G}(z_{\rm r}, z'_{\rm r}, t_{\rm r})|_{z_{\rm r}=\pm 1/2}$. Substituting the initial condition given by Equation (4), it is possible to investigate the influence of the surface viscosity on the relaxation process of the director angle when the surface easy axis is changing according to Equation (3). This completes the process of obtaining exact solutions for the problem stated in Section 2.

## 4. Relaxation and surface viscosity

In Figure 1(a), the behaviour of $\phi(z_{\rm r}, t_{\rm r})$ is shown versus $z_r$ for different values of $t_r$ to illustrate the time evolution of the profile of the director angle. The asymmetry in the spatial distribution of the director is evident for intermediate times, i.e. between the initial and the final states. The relaxation of the solution for the considered set of parameters in Figure 1(b) is also evident, where the profile of the director angle is shown for two different values of the reduced surface viscosity. Notice that these values correspond to a ratio surface to bulk viscosity $\eta_{\rm s}/\eta_{\rm b} = \upsilon d$ of the order of micrometres for typical NLC cells ($d \approx 1\ \mu$m) and they can be considered as very high when compared with the values employed in [2], which are of the order of

nanometres. In addition, the two illustrative values we are using for the reduced anchoring energy correspond to $d = 10L$ and $d = L$, where $L$ is a typical extrapolation length. These values represent, respectively, an almost strong ($u = 10$) and a relatively weak ($u = 1$) anchoring situation.

Once the exact profile of the director angle is obtained, other measurable physical properties of the NLC sample can be explored. For instance, in the case in which a linear polarised beam impinges normally on the nematic sample, the optical path difference $\Delta l$, between the ordinary and the extraordinary ray, is given by [26]

$$\Delta l = \int_{-d/2}^{d/2} \Delta n(\phi)\, dz,$$

$$\Delta n(\phi) = n_{\text{eff}}(\phi) - n_{\text{o}} = n_{\text{o}} \left\{ \frac{1}{\sqrt{1 - r \sin^2(\phi)}} - 1 \right\}, \tag{23}$$

with $r = 1-(n_{\text{o}}/n_{\text{e}})^2$, where $n_{\text{o}}$ and $n_{\text{e}}$ are the ordinary and extraordinary refractive indices, respectively. Using the results obtained in Section 4, the time dependence of $\Delta l$ can be obtained by means of [23] and some representative situations will be illustrated.

The time dependence of the time derivative of the director angle, at $z_r = 0.1$, is shown in Figure 2(a) for two different values of the dimensionless surface viscosity $\upsilon = \eta_{\text{s}}/(\eta_{\text{b}} d)$ and for significant values of the reduced anchoring energy $u_{\pm} = W_{\pm}\, d/K$, which represent a relatively strong anchoring situation for the surface placed at $z = d/2$ ($u_+ = 10$) and a very weak anchoring at $z = -d/2$ ($u_- = 1$). Even if for short times the behaviours of the director angle are similar for small ($\upsilon = 0.1$) and large ($\upsilon = 1.0$) values of the surface viscosity, the large time behaviour is very different. The relaxation behaviour of the system toward the stationary configuration of the director angle can be fast or slow according to whether the surface viscosity is small or large. The optical path difference exhibited in Figure 2(b) is shown to be highly sensitive to the variations of $\upsilon$, demonstrating its influence on the measurable physical quantities characterising the sample.

The relaxation process is therefore strongly dependent on the strength of the surface viscosity and is also affected by the relaxation times characterising the easy axes at the surfaces, as can be seen from Figure 3(a), where the quantity $\dot{\phi}(z_{\text{r}}, t_{\text{r}})|_{z_{\text{r}}=0.1}$ is shown. In Figure 3(b), we explore the behaviour of the reduced optical path difference for a set of contrasting characteristic times of the easy axis distribution at the surfaces.

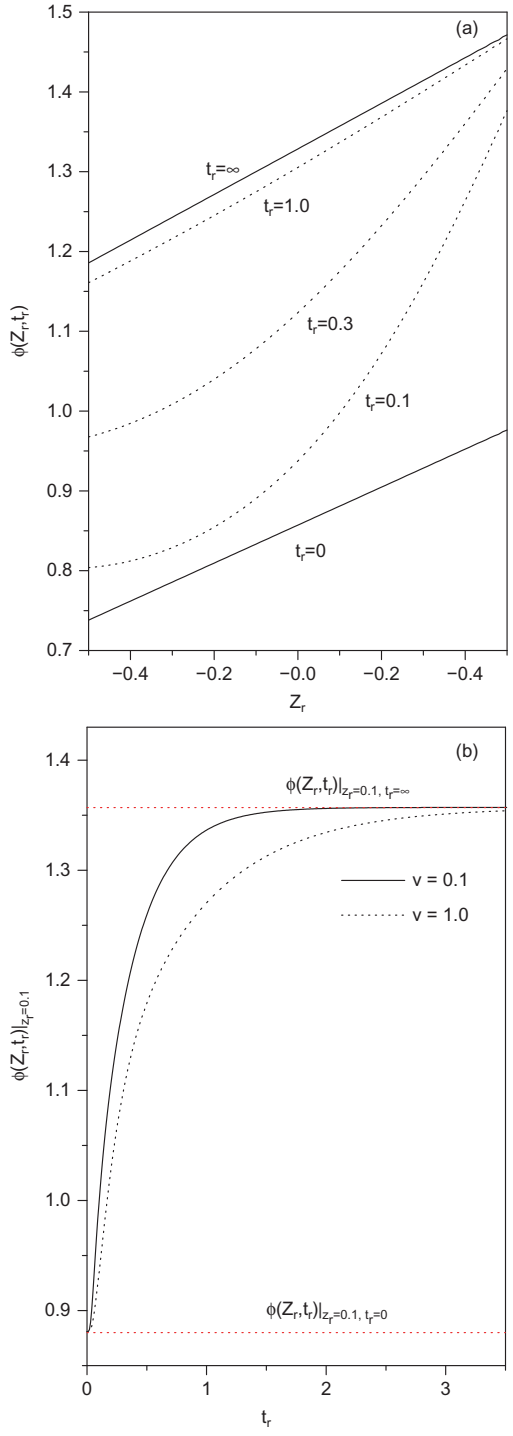


Figure 1. (a) $\phi(z_{\text{r}}, t_{\text{r}})$ versus $z_r$ for different values of $t_r$ and $\upsilon = 0.1$ to illustrate the time evolution of the director profile. The dotted lines represent the director profile for different values of $t_r$ from the initial condition to the stationary situation (solid lines). (b) $\phi(z_{\text{r}}, t_{\text{r}})\,|_{z_{\text{r}}=0.1}$ versus $t_r$ for two different values of $\upsilon$ to illustrate the influence of the viscosity on the time evolution of the director profile from the initial condition to a stationary situation (dotted lines). The curves have a horizontal slope at the origin. For both cases, we consider, for simplicity, $u_+ = 10$, $u_- = 1$, $\phi_{\text{i},+} = 1$, $\phi_{\text{i},-} = 0.5$, $\phi_{\text{f},+} = 1.5$, $\phi_{\text{f},-} = 0.9$, $\tau_{\text{r},+} = 0.01$ and $\tau_{\text{r},-} = 0.05$.

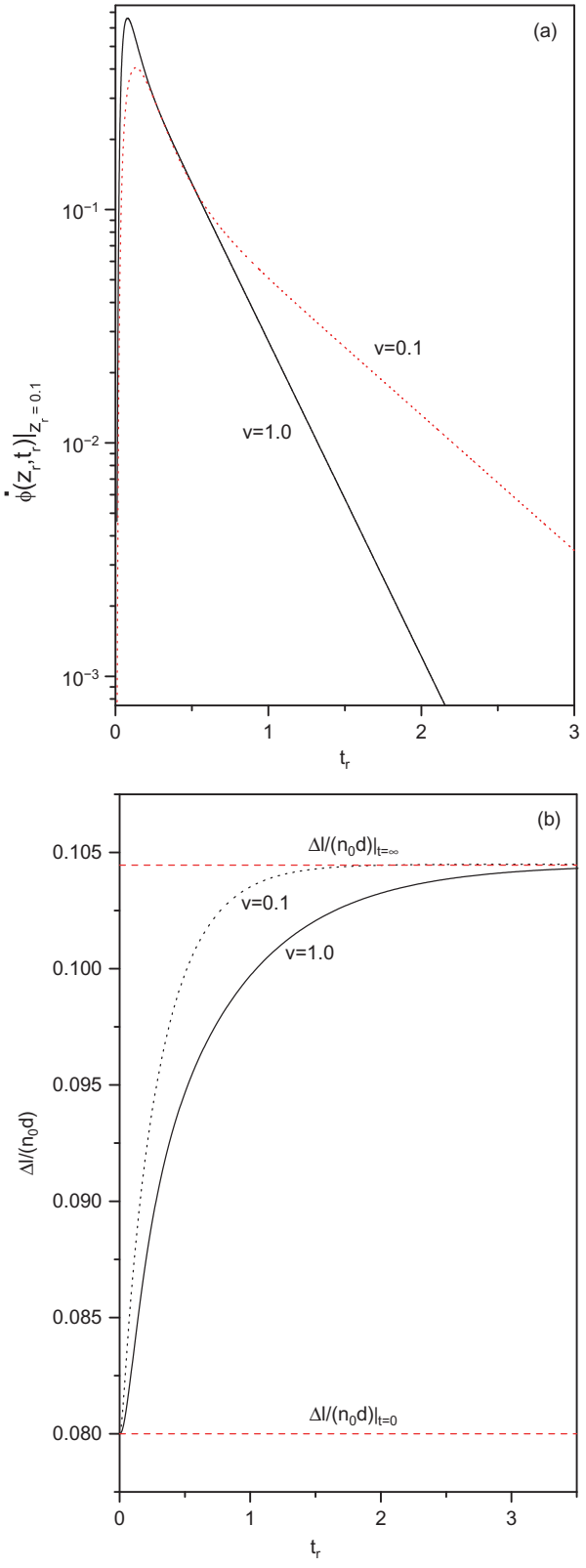


Figure 2. (a) $\dot{\phi}(z_r, t_r)|z_r = 0.1$ versus $t_r$ and (b) $\Delta l/n_0 d$ versus $t_r$ for two different values of $\upsilon$. The curves were drawn for the parameters $u_+ = 10$, $u_- = 1$, $\phi_{i,+} = 1$, $\phi_{i,-} = 0.8$, $\phi_{f,+} = 1.2$, $\phi_{f,-} = 1$ and $\tau_{r,+} = \tau_{r,-} = 0.02$.

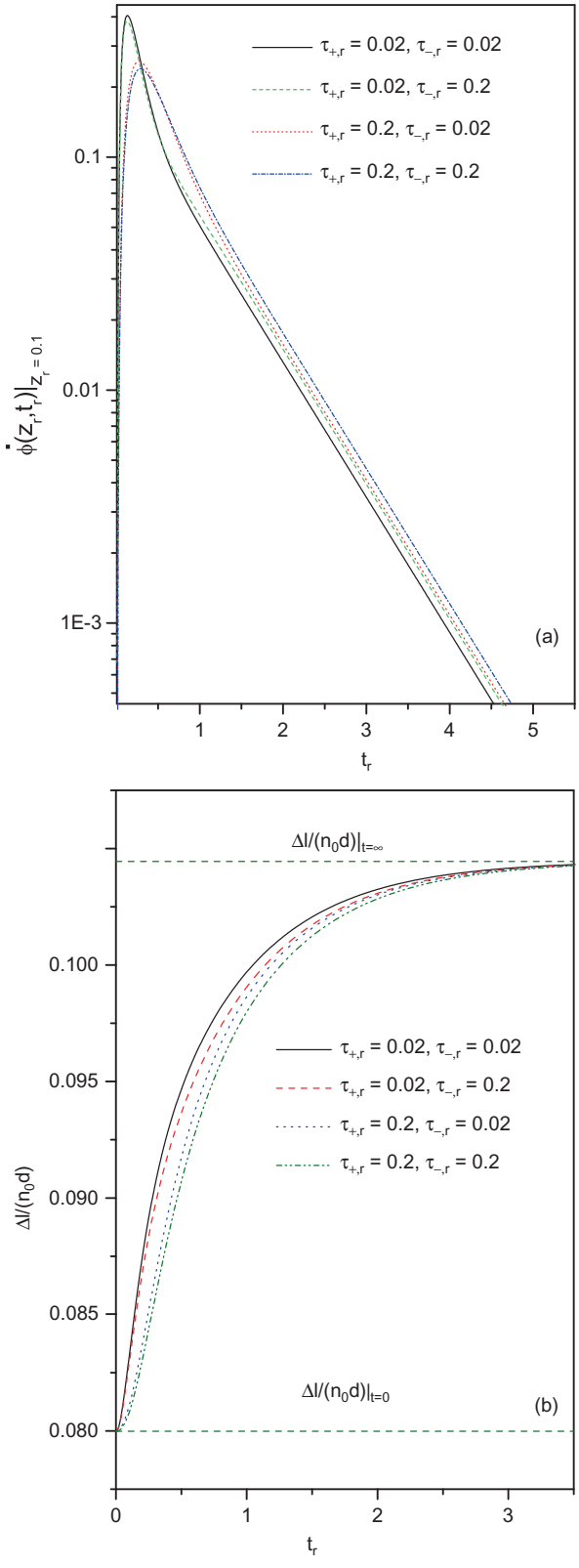


Figure 3. (a)$\dot{\phi}(z_r, t_r)|z_r = 0.1$ versus $t_r$ and (b) $\Delta l/n_0 d$ versus $t_r$ for different values of $\tau_{r,+}$ and $\tau_{r,-}$. The other parameters are $u_+ = 10$, $u_-$=1, $\phi_{i,+} = 1$, $\phi_{i,-} = 0.8$, $\phi_{f,+} = 1.2$, $\phi_{f,-} = 1$ and $\upsilon = 1.0$ (colour version online).

As expected, this quantity is directly affected by the variations of the characteristic times and changes monotonically between two limiting values corresponding to the initial and stationary configurations.

In the same direction, the influence of the anchoring energy on the relaxation process can be appreciated in Figure 4(a). At a first glance, Figures 2(a) and 4(a) have similar trends. However, while Figure 4(a) shows that the relaxation process is fast for *large* values of the reduced anchoring, Figure 2 exhibits a fast behaviour for *small* values of the surface viscosity. Accordingly, the slow relaxation behaviour is exhibited for *small* values of the anchoring strength (i.e. for weak anchoring) and for *large* values of the surface viscosity. As is evident from Figure 4(b), the optical path difference is also strongly affected by the asymmetry in the conditions of the surfaces limiting the sample.

## 5. Electric field effect

Let us now investigate the effects produced on the relaxation of the system by a constant electric field applied to the sample. In particular, the results found below may be useful to analyse the system subjected to a time-dependent field [12] for time intervals that are very small when compared to the typical characteristic times related to relaxation of the electric field. In this context, the equation to be considered, in dimensionless form, to obtain the behaviour of the twist angle in the presence of a constant electric field is given by

$$\frac{\partial}{\partial t_{\mathrm{r}}}\phi_E\left(z_{\mathrm{r}},t_{\mathrm{r}}\right)=\frac{\partial^2}{\partial z_{\mathrm{r}}^2}\phi_E\left(z_{\mathrm{r}},t_{\mathrm{r}}\right)-\frac{1}{\lambda^2}\phi_E\left(z_{\mathrm{r}},t_{\mathrm{r}}\right), \quad (24)$$

where $\lambda=1/E_0\sqrt{k/\left(\varepsilon_a d^2\right)}$. The external field considered here is $\mathbf{E}=E_0\mathbf{z}$ and the dielectric anisotropy of the NLC is assumed to be positive ($\varepsilon_a=\varepsilon_{||}-\varepsilon_{\perp}$, where $||$ and $\perp$ refer to $\mathbf{n}$). Note also that Equation (24) is obtained in the context of the small-angle approximation with weak fields. For this reason, we consider in our analysis that $\lambda\gg 1$, which corresponds to weak fields. Equation (24) has to be solved by considering the boundary conditions given by Equation (9), which contain the effect of the surface viscosity on the director angle. In order to avoid the problem of compatibility between the time derivative of the director angle on the surface and in the bulk, we consider the initial condition

$$\Phi_{E,\mathrm{i}}(z_{\mathrm{r}})=\mathcal{A}_{E,\mathrm{i}}e^{z/\lambda}+\mathcal{B}_{E,\mathrm{i}}e^{-z/\lambda}, \quad (25)$$

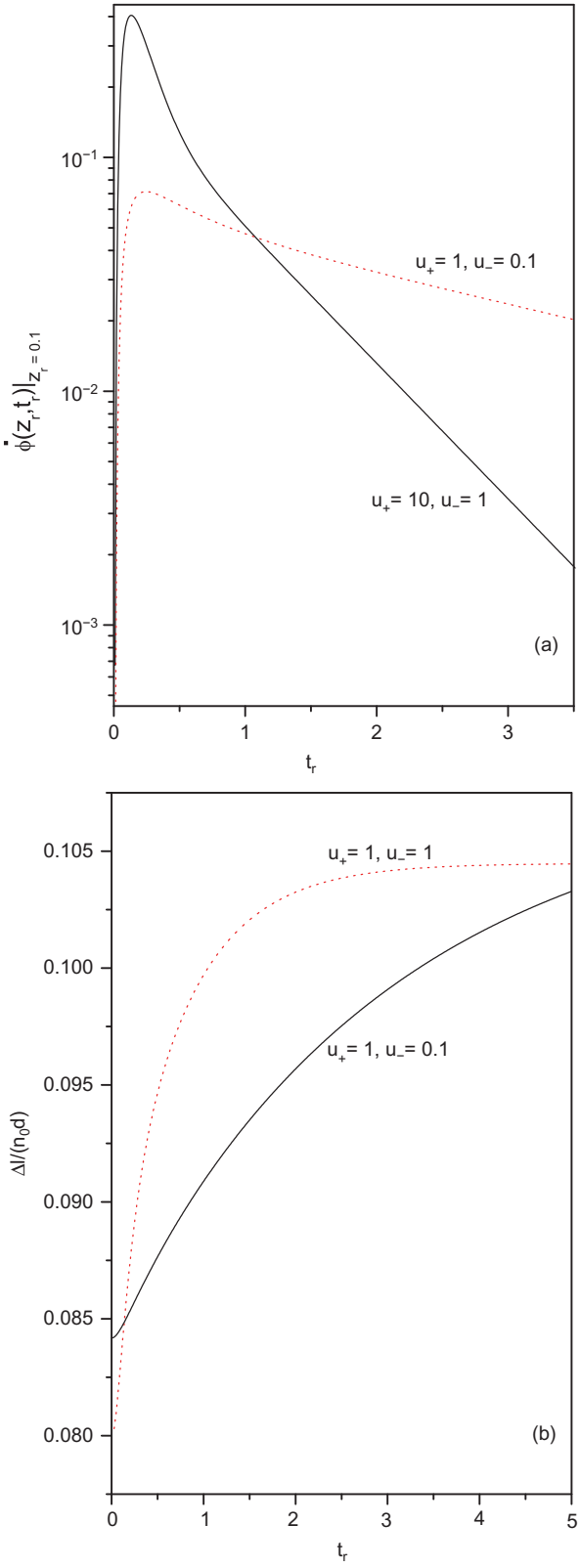


Figure 4. (a) $\dot{\phi}(z_{\mathrm{r}},t_{\mathrm{r}})|z_{\mathrm{r}}=0.1$ versus $t_r$ and (b) $\Delta l/n_0 d$ versus $t_r$ for two different values of $u_+$ and $u_-$. These curves were drawn for $\phi_{\mathrm{i},+}=1$, $\phi_{\mathrm{i},-}=0.8$, $\phi_{\mathrm{f},+}=1.2$, $\phi_{\mathrm{f},-}=1$, $\upsilon=1$ and $\tau_{\mathrm{r},+}=\tau_{\mathrm{r},-}=0.02$.

with

$$\mathcal{A}_{E,\mathrm{i(f)}} = \frac{u_+\lambda(1+u_-\lambda)\phi_{\mathrm{i(f)},+}e^{\frac{1}{2\lambda}} + u_-\lambda(1+u_+\lambda\phi_{\mathrm{i(f)},-})e^{-\frac{1}{2\lambda}}}{(1+u_-\lambda)(1+u_+\lambda)e^{\frac{1}{\lambda}} - (1-u_-\lambda)(1-u_+\lambda)e^{-\frac{1}{\lambda}}},$$

$$\mathcal{B}_{E,\mathrm{i(f)}} = \frac{u_-\lambda(1+u_+\lambda)\phi_{\mathrm{i(f)},-}e^{\frac{1}{2\lambda}} + u_+\lambda(1+u_-\lambda\phi_{\mathrm{i(f)},+})e^{-\frac{1}{2\lambda}}}{(1+u_-\lambda)(1+u_+\lambda)e^{\frac{1}{\lambda}} - (1-u_-\lambda)(1-u_+\lambda)e^{-\frac{1}{\lambda}}}. \tag{26}$$

Equation (25) is obtained by solving the equation

$$\frac{d^2}{dz_\mathrm{r}^2}\Phi_E(z_\mathrm{r}) - \frac{1}{\lambda^2}\Phi_E(z_\mathrm{r}) = 0, \tag{27}$$

with the boundary condition

$$\pm\frac{d}{dz_\mathrm{r}}\Phi_E(z_\mathrm{r}) + u_\pm(\Phi_E(z_\mathrm{r}) - \phi_{\mathrm{i},\pm})\Big|_{z_\mathrm{r}=\pm 1/2} = 0. \tag{28}$$

Similarly to the previous case, discussed in the absence of an electric field, we have a stationary configuration of the director angle which is given by

$$\Phi_{E,\mathrm{f}}(z_\mathrm{r}) = \mathcal{A}_{E,\mathrm{f}}e^{z/\lambda} + \mathcal{B}_{E,\mathrm{f}}e^{-z/\lambda}. \tag{29}$$

It is worth mentioning that the initial condition given by Equation (25) satisfies the condition of compatibility given by Equation (7), i.e. for $t = 0$ the time derivative of the director angle on the surface and in the bulk are the same.

Following the procedure employed in Section 3, we use the Green function approach to solve Equation (24). After some calculations, it is possible to show that the solution for this case is given by

$$\begin{aligned}\phi_E(z'_\mathrm{r}, t) = &-\int_{-1/2}^{1/2} dz_\mathrm{r}\Phi_E(z_\mathrm{r})\mathcal{G}(z_\mathrm{r}, z'_\mathrm{r}, t)e^{-t/\lambda^2}\\ &-\int_0^t dt' e^{-(t-t')/\lambda^2}\left[u_+\phi_{\mathrm{s},+}(t')\tilde{\mathcal{G}}_{E,+}(z'_\mathrm{r}, t-t')\right.\\ &\left.+\,u_-\phi_{\mathrm{s},-}(t')\tilde{\mathcal{G}}_{E,-}(z'_\mathrm{r}, t-t')\right]\\ &-\upsilon\left[\,\Phi_E(z_\mathrm{r})|_{z_\mathrm{r}=\frac{1}{2}}\,\tilde{\mathcal{G}}_{E,+}(z'_\mathrm{r}, t)\right.\\ &\left.+\Phi_E(z_\mathrm{r})|_{z_\mathrm{r}=-\frac{1}{2}}\,\tilde{\mathcal{G}}_{E,-}(z'_\mathrm{r}, t)\right],\end{aligned} \tag{30}$$

with $\tilde{\mathcal{G}}_{E,\pm}(z'_\mathrm{r}, t_\mathrm{r}) = \mathcal{G}_E(z_\mathrm{r}, z'_\mathrm{r}, t_\mathrm{r})\Big|_{z_\mathrm{r}=\pm 1/2}$ and the Green function is given by

$$\begin{aligned}\mathcal{G}_E(z_\mathrm{r}, z'_\mathrm{r}; t_\mathrm{r}) = -\sum_{n=1}^{\infty}\frac{e^{-k_n^2 t_\mathrm{r}}}{k_n\tilde{\mathcal{F}}(k_n)}&\left\{k_n\cos\left[k_n\left(\frac{1}{2}+z_\mathrm{r}\right)\right]\right.\\ &\left.+\left(u_- - \frac{\upsilon}{\lambda^2} - \upsilon k_n^2\right)\sin\left[k_n\left(\frac{1}{2}+z_\mathrm{r}\right)\right]\right\}\\ &\times\left\{k_n\cos\left[k_n\left(\frac{1}{2}-z'_\mathrm{r}\right)\right]\right.\\ &\left.+\left(u_+ - \frac{\upsilon}{\lambda^2} - \upsilon k_n^2\right)\sin\left[k_n\left(\frac{1}{2}-z'_\mathrm{r}\right)\right]\right\},\end{aligned} \tag{31}$$

for $-1/2 \le z_\mathrm{r} < z'_\mathrm{r}$, and

$$\begin{aligned}\mathcal{G}_E(z_\mathrm{r}, z'_\mathrm{r}; t_\mathrm{r}) = -\sum_{n=1}^{\infty}\frac{e^{-k_n^2 t_\mathrm{r}}}{k_n\tilde{\mathcal{F}}(k_n)}&\left\{k_n\cos\left[k_n\left(\frac{1}{2}+z'_\mathrm{r}\right)\right]\right.\\ &\left.+\left(u_- - \frac{\upsilon}{\lambda^2} - \upsilon k_n^2\right)\sin\left[k_n\left(\frac{1}{2}+z'_\mathrm{r}\right)\right]\right\}\\ &\times\left\{k_n\cos\left[k_n\left(\frac{1}{2}-z'_\mathrm{r}\right)\right]\right.\\ &\left.+\left(u_+ - \frac{\upsilon}{\lambda^2} - \upsilon k_n^2\right)\sin\left[k_n\left(\frac{1}{2}-z'_\mathrm{r}\right)\right]\right\},\end{aligned} \tag{32}$$

for $z'_\mathrm{r} < z_\mathrm{r} \le 0$, where

$$\begin{aligned}\tilde{\mathcal{F}}_E(k_n) = \frac{1}{2k_n}&\left[k_n^2\left(1+\upsilon\left(6+u_+ + u_- - \frac{2}{\lambda^2} - \upsilon k_n^2\right)\right)\right.\\ &\left.-\left(u_+ - \frac{1}{\lambda^2}\right)\left(1+u_- - \frac{1}{\lambda^2}\right) + \frac{1}{\lambda^2} - u_-\right]\cos(k_n)\\ &+\frac{1}{2}\left[2+u_+ + u_- - \frac{2}{\lambda^2}\right.\\ &\left.+2\left(u_+ + u_- - \frac{2}{\lambda^2} - k_n^2\right) - 4k_n^2\upsilon^2\right]\sin(k_n).\end{aligned} \tag{33}$$

The $k_n$ are obtained from the equation

$$\left(\mathcal{U}_+\mathcal{U}_- - k_n^2\right)\sin(k_n) + k_n\left(\mathcal{U}_+ + \mathcal{U}_-\right)\cos(k_n) = 0, \tag{34}$$

where $\mathcal{U}_+ = u_+ - \upsilon/\lambda^2 - \upsilon k_n^2$ and $\mathcal{U}_- = u_- - \upsilon/\lambda^2 - \upsilon k_n^2$.

Figure 5(a) shows the profile for different times in order to illustrate the effect produced by the electric field. The system relaxes from an initial configuration given by Equation (25) to a stationary configuration which is given by Equation (29). In Figure 5(b), we illustrate the behaviour of the time derivative of the director angle in the presence and in the absence of an electric field for an arbitrary value of $\upsilon$. Note that for small times, i.e. $t_\mathrm{r} \ll 1$, Figure 5(b) shows that the effect of the electric field is not verified as compared to the situation where it is absent (long dashed line). This feature may be an indication that considering an

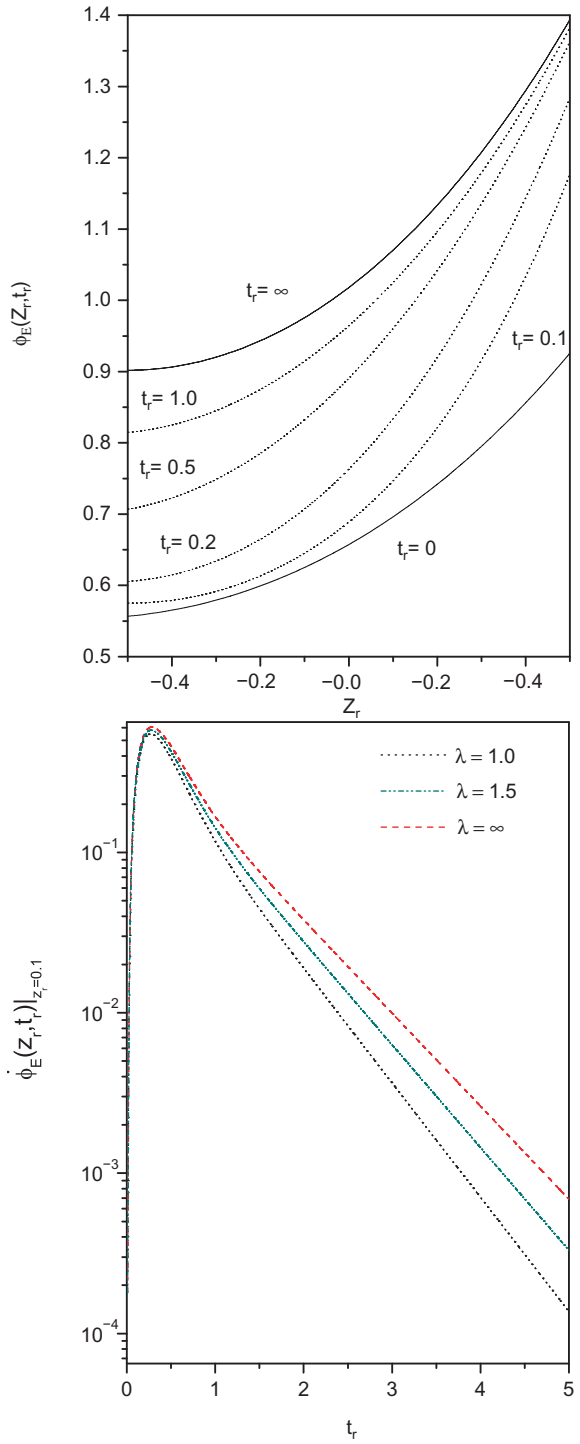


Figure 5. (a) $\phi_E(z_r, t_r)$ versus $z_r$ for different values of $t_r$ and $\lambda = 1$ to illustrate the time evolution of the director profile. The dotted lines represent the director profile for different values of $t_r$ from the initial condition to the stationary situation (solid lines). (b) $\dot{\phi}_E(z_r, t_r)|_{z_r=0.1}$ versus $t_r$ for $\lambda = 1$, $\lambda = 1.5$, and $\lambda = \infty$ to illustrate the influence of the electric field on the relaxation of the director profile. For both cases, we consider, for simplicity, $u_+ = 10$, $u_- = 1$, $\phi_{i,+} = 1$, $\phi_{i,-} = 0.5$, $\phi_{f,+} = 1.5$, $\phi_{f,-} = 0.9$, $\tau_{r,+} = 0.2$, $\upsilon = 1$ and $\tau_{r,-} = 0.1$ (colour version online).

electric field with a small characteristic time is useful so as to avoid the compatibility problem between the time derivative of the director angle on the surface and in the bulk, as discussed in [7–10], without significant changes on the relaxation of the profile.

## 6. Concluding remarks

These fundamental equations and the exact results we have obtained permit us to develop the entire analysis of the dynamics of the molecular orientation–reorientation in a cell characterized by time-dependent boundary conditions, taking into account the effect of the surface viscosity and the anchoring energy. This analysis we have presented is a quite general approach to face the problem of interpreting experimental results for which the consideration of the role of surface viscosity is relevant. In addition, our approach shows that an incompatibility of the initial derivative of the director angle on the bounding surface does not arise when it is deduced from the bulk or from the surface dynamic equations, because the problem is stated in such a manner so that the appropriate initial conditions on this first derivative are considered. The exact Green function approach we have developed permits us to obtain a closed expression for the space-time profile of the director angle and for the temporal dependence of the optical path difference of a typical NLC cell. All these calculations have been performed by taking into account easy axis distributions that are time dependent. This kind of analysis can find applications in liquid-crystalline systems for which light-induced easy directions are induced in view of the presence of dyes. In the analysis presented above, the anchoring energies have been assumed to be time independent. In the case where the easy direction is modified optically, the anchoring energy strengths also depend on time. In this framework, the analysis reported above has to be modified by taking into account in the boundary conditions in Equation (2) that also $W_\pm = W_\pm(t)$, in such a manner that the time evolution of the nematic orientation is continuous in time, without discontinuity at the border. Work is in progress along these lines and will be published elsewhere.

## Acknowledgements

We are grateful to Giovanni Barbero (Italy) for very fruitful discussions. This work was partially supported by the National Institutes of Science and Technology in Complex Systems (E.K. Lenzi) and Complex Fluids (L.R. Evangelista), CNPq, Brazil.

## References


[1] Petrov, A.G.; Ionescu, A.Th.; Versace, C.; Scaramuzza, N. *Liq. Cryst*. **1995**, *19*, 169–178.

[2] Mertelj, A.; Copic, M. *Phys. Rev. Lett.* **1998**, *81*, 5844–5847.

[3] Faetti, S.; Nobili, M.; Raggi, I. *Eur. Phys. J.B* **1999**, *11*, 445–453.

[4] Marinov, Y.; Shonova, N.; Versace, C.; Petrov, A.G. *Mol. Cryst. Liq. Cryst*. **1999**, *329*, 533–538.

[5] Marinov, Y.; Shonova, N.; Naydenova, N.; Petrov, A.G. *Mol. Cryst. Liq. Cryst*. **2000**, *351*, 411–417.

[6] Mertelj, A.; Copic, M. *Phys. Rev. E* **2000**, *61*, 1622–1628.

[7] Durand, G.E.; Virga, E.G. *Phys. Rev. E* **1999**, *59*, 4137–4142.

[8] Sonnet, A.; Virga, E.G.; Durand, G.E. *Phys. Rev. E* **2000**, *62*, 3694–3701.

[9] Barbero, G.; Dahl, I.; Komitov, L. *J. Chem. Phys.* **2009**, *130*, 174902

[10] Barbero, G.; Pandolfi, L. *Phys. Rev. E* **2009**, *79*, 051701.

[11] Alexe-Ionecu, A.L.; Barbero, G.; Komitov, L. *Phys. Rev. E* **2009**, *77*, 051701.

[12] Lenzi, E.K.; Barbero, G. *Eur. Phys. Lett*. **2009**, *88*, 58003.

[13] Derzhanskii, A.I.; Petrov, A.G. *Acta Phys. Pol. A* **1979**, *55*, 747.

[14] Rapini, A.; Papoular, M.J. *Phys. (Paris), Colloq*. **1969**. *30*, C4–54.

[15] Sonin, A.A. *The Surface Physics of Liquid Crystals*; Gordon and Breach: Philadelphia, 1995.

[16] Barbero, G.; Lenzi, E.K. *Phys. Lett. A* **2010**, *374*, 1565–1569.

[17] Alexe-Ionescu, A.L.; Uncheselu, C.; Lucchetti, L.; Barbero, G. *Phys. Rev. E* **2007**, *75*, 021701.

[18] Fedorenko, D.; Slyusarenko, K.; Ouskova, E.; Reshetnyak, V.; Ha, K.; Karapinar, R.; Reznikov, Y. *Phys. Rev. E* **2008**, *77*, 061705.

[19] Pieranski, P.; Jerome, B.; Gabay, M. *Mol. Cryst. Liq. Cryst*. **1990**, *179*, 285–315.

[20] Kuksenok, O.V.; Shianovskii, S. *Mol. Cryst. Liq. Cryst*. **2001**, *359*, 427–438.

[21] Janossy, I. *Phys. Rev. E* **1994**, *49*, 2957–2963.

[22] Francescangeli, O.; Slussarenko, S.; Simoni, F.; Andrienko, D.; Reshetnyak, V.; Reznikov, Y. *Phys. Rev. Lett*. **1999**, *82*, 1855–1858.

[23] Ouskova, E.; Fedorenko, D.; Reznikov, Y.; Shiyanovskii, S.V.; Su, L.; West, J.L.; Kuksenok, O.V.; Francescangeli, O.; Simoni, F. *Phys. Rev. E* **2001**, *63*, 021701.

[24] Ouskova, E.; Reznikov, Y.; Shiyanovskii, S.V.; Su, L.; West, J.L.; Kuksenok, O.V.; Francescangeli, O.; Simoni, F. *Phys. Rev. E* **2001**, *64*, 051709.

[25] Virga, E.G. *Variational Theories for Liquid Crystals*; Chapman and Hall: London, 1994.

[26] Barbero, G.; Barberi, R. In *The Physics of Liquid Crystalline Materials*: Khoo, I.C., Simoni, F., Eds.; Gordon and Breach: London, 1988.